DFT Study of Solvent Coordination Effects on Titanium-Based Epoxidation Catalysts. Part Two: Reactivity of Titanium Hydroperoxo Complexes in Ethylene Epoxidation

Robert R. Sever and Thatcher W. Root*

Department of Chemical Engineering, University of Wisconsin-Madison, 1415 Engineering Drive, Madison, Wisconsin 53706

Received: May 2, 2002; In Final Form: February 3, 2003

Density functional theory has been used to study the effects of solvent coordination on the reactivity of titanium hydroperoxo complexes in the epoxidation of the model olefin ethylene. Complexes possessing a variety of coordination environments have been modeled with unconstrained single coordination sphere clusters using a B3LYP/ECP methodology. The Gibbs free energy of activation for ethylene epoxidation with a nonligated titanium hydroperoxo species is 25.7 kcal/mol. Addition of a single solvent ligand to the titanium center has little effect on the activation barrier unless that ligand participates in a hypervalent ω bond with the proximal oxygen (Oα) of the hydroperoxo moiety; in that case, the ω bond inhibits the heterolytic cleavage of the Ti−Oα bond and increases the activation barrier for transfer of Oα to ethylene by 6−7 kcal/mol. Hydrogen bonding of the hydroperoxo moiety with a protic solvent ligand via a monodentate five-membered ring structure does not enhance the reactivity of the titanium hydroperoxo complex. The presence of two solvent ligands on the titanium center increases the activation barrier 11−16 kcal/mol by sterically hindering the attack of ethylene at Oα. The activation barrier is not affected by the presence of a hydrogen-bonded protic solvent molecule bridging the hydroperoxo moiety and a protic ligand on titanium. NBO analysis indicates that changes in the electrophilicity of the peroxo group caused by solvent coordination do not control the observed reactivity of the titanium hydroperoxo complexes. The activation barriers for ethylene epoxidation with titanium hydroperoxo, methylperoxo, and trifluoromethylperoxo oxidants decrease with increasing positive charge on the atom bonded to the distal peroxo oxygen (Oβ) through stabilization of the developing negative charge on Oβ. Comparison of the Gibbs activation barriers for the formation of the titanium hydroperoxo intermediate and its subsequent reaction with ethylene indicates that the oxygen transfer step is the rate-determining step for the overall epoxidation mechanism.

Introduction

This report continues our exploration of solvent coordination effects on the performance of titanium-based epoxidation catalysts. The heterogeneous Ti(IV)−H_2O_2 oxidation system has received much attention for its potential to replace environmentally harmful stoichiometric or homogeneously catalyzed epoxidation processes. Experiments have shown that solvent identity can have a pronounced effect on the activity and selectivity of titanium-based catalysts in liquid-phase epoxidation reactions.[1−9] Fundamental understanding of these solvent effects currently remains limited. In our previous paper,[10] we summarized the effects of solvent coordination on the formation and structure of the titanium hydroperoxo (TiOOH) species thought to be the active oxidizing intermediate in the Ti(IV)−H_2O_2 system. Our results demonstrated the probable existence of several degenerate titanium hydroperoxo species possessing monodentate (η^1) or bidentate (η^2) hydroperoxo moieties and a single water ligand coordinating the titanium center. Protic molecules were shown to facilitate the proton transfer reaction that generates the titanium hydroperoxo intermediate. As a result, the intermediate may be formed with a protic molecule bridging the hydroperoxo moiety and the water ligand via hydrogen-bonding interactions as shown schematically in Figure 1.

In the case of hydrophobic titanium-based catalysts, olefin epoxidation rates are generally higher in protic solvents (e.g., methanol or ethanol) than in aprotic solvents (e.g., acetonitrile or acetone).[1−6] To explain this trend, Clerici and co-workers[2,11] proposed the existence of a five-membered ring titanium hydroperoxo intermediate in which a protic solvent ligand on the titanium center donates a hydrogen bond to the distal oxygen of the hydroperoxo moiety (Figure 2). According to their proposal, hydrogen bonding in the five-membered ring enhances epoxidation reaction rates by either stabilizing the formation of the titanium hydroperoxo intermediate or increasing its electrophilicity. Recent computational studies[10,12,13] have demonstrated that the five-membered ring intermediate is not significantly more stable than other titanium hydroperoxo complexes possessing a single protic ligand on titanium. In this

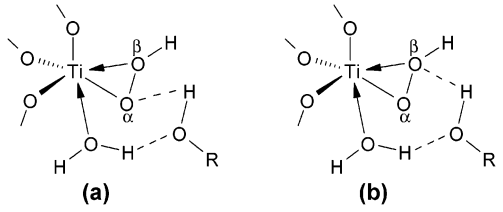

Figure 1. Schematic representation of the hydrogen-bonded bridging interaction in which a protic molecule ROH simultaneously receives a hydrogen bond from a water ligand on titanium and donates a hydrogen bond to either the (a) proximal or (b) distal oxygen of the hydroperoxo group. (Arrow indicates coordinative interaction with titanium; dashed line indicates hydrogen-bonding interaction.)

* To whom correspondence should be addressed. E-mail: thatcher@engr.wisc.edu.

10.1021/jp026057k CCC: $25.00
Published on Web 04/02/2003

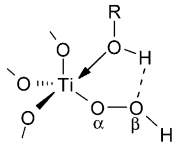

Figure 2. Schematic representation of the hydrogen-bonded five-membered ring titanium hydroperoxo intermediate proposed by Clerici and co-workers.[2,11]

report, we examine the reactivity of several titanium hydroperoxo intermediates, including the proposed five-membered ring complex.

Several researchers have studied the epoxidation of the model olefin ethylene with titanium hydroperoxo species using Hartree−Fock and density functional theory.[14−20] Few of these studies have determined transition states and activation barriers for models of the titanium active site that include coordinated solvent molecules.[17,18,20] Yudanov et al.[18] calculated activation barriers of 12.7 and 12.4 kcal/mol for the epoxidation of ethylene with the model titanium hydroperoxo clusters $Ti(OH)_3(OOH)$ and $Ti(OH)_3(OOH)\cdot NH_3$, respectively. They concluded that solvent ligands on the titanium site have little effect on the reactivity of titanium hydroperoxo species. Tantanak et al.[17] calculated an 11.9 kcal/mol activation barrier for ethylene epoxidation with an unconstrained $Ti(OSiH_3)_3(OOH)\cdot$MeOH cluster in which the methanol ligand does not form a five-membered ring with the hydroperoxo moiety. They did not compare their results with a nonligated titanium hydroperoxo species. Additional investigation is clearly needed to ascertain the role of local interactions between solvent molecules and the active site in the experimentally observed solvent effects for the Ti(IV)−H_2O_2 epoxidation system. We report here the first comprehensive computational study of solvent coordination effects on the reactivity of titanium hydroperoxo complexes in ethylene epoxidation.

Computational Methodology

All calculations reported here were performed with Gaussian 98[21] and NBO version 5.0[22] software. Density functional theory as implemented in the restricted B3LYP hybrid exchange-correlation scheme was used to include some effects of electron correlation with only a marginal increase in computational cost over Hartree−Fock methods. All results have been obtained for cluster geometries optimized in the gas phase. Solvent continuum effects have been considered for selected cases using the gas-phase optimized geometries in conjunction with the integral equation formalism of the polarizable continuum model (IEF−PCM).[23] All stationary points have been characterized with a full vibrational analysis, and all reported energy differences include zero-point energy corrections. Thermochemistry calculations have been performed at standard temperature and pressure in order to elucidate entropy effects on solvent coordination and activation barriers. The zero-point energy corrections and thermochemistry results (ΔH, ΔS, and ΔG) have not been scaled. Except where noted, a LANL2DZ effective core potential was used to represent titanium, and a 6-311+G(d,p) basis set was used for all other atoms. Similar computational methods have been shown to yield accurate geometries and energies for similar titanium species.[18,24] Natural bond orbital (NBO) methods were used to analyze the resultant wave functions in terms of optimally chosen, localized orbitals corresponding to a Lewis structure representation of chemical bonding.[25] The occupancies of natural bond orbitals are highly condensed in the most important one-center (lone pair) and two-center (bond) members, allowing electron delocalization effects, or donor−acceptor interactions, to be treated with standard perturbative techniques.

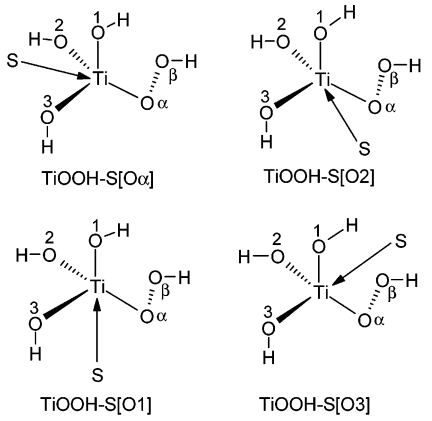

Figure 3. Nomenclature for the orientation of a solvent ligand (S) with respect to the hydroperoxo moiety in a $Ti(OH)_3(OOH)$ complex. The solvent ligand is positioned on the face of the $Ti(OH)_3(OOH)$ tetrahedron opposite the proximal hydroperoxo oxygen Oα or the hydroxyl oxygen O1, O2, or O3. TiOOH−S[O3] is distinguished from TiOOH−S[O1] and TiOOH−S[O2] by having the solvent ligand positioned on the same face of the $Ti(OH)_3(OOH)$ tetrahedron as the distal hydroperoxo oxygen (Oβ).

For most calculations, the titanium hydroperoxo intermediate was modeled with unconstrained $Ti(OH)_3(OOH)$ clusters representing the first coordination sphere of the titanium active site. A thorough discussion of the advantages and limitations of this model is provided in our previous paper.[10] An actual titanium-based epoxidation catalyst generally possesses two, three, or four Ti−O−Si bonds to a siliceous framework or support. The hydroxyl groups in our cluster model therefore may represent either bonds to framework silicon atoms (Ti−O−Si modeled as Ti−O−H) or hydrolyzed framework linkages. Four different solvent molecules—water, ammonia, methanol, and acetonitrile—were added to this cluster as ligands on titanium. We have numbered the three nonreactive structural hydroxyl groups in $Ti(OH)_3(OOH)$ to help distinguish the four possible orientations of solvent ligands with respect to the hydroperoxo group (see Figure 3). A solvent ligand may coordinate the titanium center in a position trans to the proximal hydroperoxo oxygen Oα or trans to hydroxyl oxygen O1, O2, or O3. We have also optimized $Ti(OH)_3(OOH)$ clusters in which a protic solvent molecule ROH simultaneously receives a hydrogen bond from a ligand on titanium and donates a hydrogen bond to either the proximal (Oα) or distal (Oβ) oxygen of the hydroperoxo group. These hydrogen-bonded bridging positions will be referred to as HB-α and HB-β and are shown schematically in parts a and b of Figure 1, respectively. Larger hydrogen-bonded networks involving multiple protic species are beyond the scope of the present study. The optimized titanium hydroperoxo clusters will be labeled as TiOOH(η^1 or η^2)−(νS[O#], ROH[HB-α or HB-β]) where η^1 or η^2 denotes monodentate or bidentate coordination of the hydroperoxo moiety to the titanium center, ν (0, 1, or 2) is the number of solvent (S) ligands coordinating the titanium atom, O# is the label of the oxygen positioned trans to the solvent ligand, and ROH[HB-α or HB-β] indicates the presence of a protic solvent molecule in either of the aforementioned bridging positions.

To further elucidate the factors controlling the reactivity of titanium peroxo complexes, the model oxidants $Ti(OH)_3(OOCH_3)$ and $Ti(OH)_3(OOCF_3)$ have also been studied. The nonligated titanium methylperoxo and trifluoromethylperoxo

TABLE 1: Activation Barriers and Reaction Energies for the Epoxidation of Ethylene with Titanium Hydroperoxo Intermediates Possessing Various Coordination Environments (in kcal/mol)

	activation barrier				reaction energy	
epoxidation reaction	ΔE_A	ΔH_A	$T\Delta S_A$	ΔG_A	ΔE_R	ΔG_R
$TiOOH(\eta^2) + C_2H_4 \rightarrow TiOH + C_2H_4O$	14.8	14.3	−11.4	25.7	−44.7	−45.5
$TiOOH(\eta^1)-H_2O[O1/O2] + C_2H_4 \rightarrow TiOH-H_2O + C_2H_4O$	13.1	12.3	−12.5	24.8	−47.4	−46.9
$TiOOH(\eta^2)-H_2O[O1] + C_2H_4 \rightarrow TiOH-H_2O + C_2H_4O$	14.5	14.0	−11.4	25.3	−46.0	−46.4
$TiOOH(\eta^2)-H_2O[O2] + C_2H_4 \rightarrow TiOH-H_2O + C_2H_4O$	13.0	12.5	−11.7	24.2	−47.6	−47.4
$TiOOH(\eta^1)-H_2O[O3] + C_2H_4 \rightarrow TiOH-H_2O + C_2H_4O$	14.3	13.7	−11.5	25.2	−46.3	−46.6
$TiOOH(\eta^2)-(H_2O[O1], H_2O[O2]) + C_2H_4 \rightarrow TiOH-2H_2O + C_2H_4O$	28.4	27.5	−12.5	40.0	−42.8	−44.7
$TiOOH(\eta^1)-(H_2O[O\alpha], H_2O[O2]) + C_2H_4 \rightarrow TiOH-2H_2O + C_2H_4O$	24.4	23.5	−12.9	36.4	−44.3	−45.1
$TiOOH(\eta^2)-(H_2O[O1], H_2O[HB\text{-}\alpha]) + C_2H_4 \rightarrow TiOH-(H_2O, H_2O[HB]) + C_2H_4O$	15.3	15.0	−11.0	25.9	−45.9	−46.2
$TiOOH(\eta^2)-(H_2O[O1], H_2O[HB\text{-}\beta]) + C_2H_4 \rightarrow TiOH-(H_2O, H_2O[HB]) + C_2H_4O$	13.5	12.7	−12.5	25.2	−47.7	−47.2
$TiOOH(\eta^2)-(H_2O[O1], H_2O[O2], H_2O[HB\text{-}\alpha]) + C_2H_4 \rightarrow TiOH-(2H_2O, H_2O[HB]) + C_2H_4O$	25.3	23.9	−13.4	37.3	−43.2	−44.1
$Ti(OSiH_3)_3(OOH)(\eta^2) + C_2H_4 \rightarrow Ti(OSiH_3)_3(OH) + C_2H_4O$	15.2	14.7	−11.2	25.9	−46.2	−47.8
$Ti(OSiH_3)_3(OOH)(\eta^2)-H_2O[O1] + C_2H_4 \rightarrow Ti(OSiH_3)_3(OH)-H_2O + C_2H_4O$	13.8	13.3	−11.7	24.9	−46.3	−46.6
$Ti(OSiH_3)_3(OOH)(\eta^2)-H_2O[O3] + C_2H_4 \rightarrow Ti(OSiH_3)_3(OH)-H_2O + C_2H_4O$	13.6	13.3	−11.8	25.1	−46.4	−46.4

clusters will be abbreviated as $TiOOCH_3$ and $TiOOCF_3$, respectively.

Transition states have been calculated for the reaction of ethylene with $Ti(OH)_3(OOR)$ intermediates (R = H, CH_3, or CF_3) for a number of different cases. The optimized transition-state clusters will be referred to as TS−TiOOR(η^1 or η^2)−(νS[O#], ROH[HB-α or HB-β]), using the reactant nomenclature. The existence of a single negative vibrational mode was confirmed for each optimized transition-state structure, and intrinsic reaction coordinate calculations were used to verify the reactants and products corresponding to that mode.[26] Unless noted otherwise, activation barriers have been calculated as the difference between the energy of the transition state and the energies of the ethylene and $Ti(OH)_3(OOR)$ reactants at infinite separation. Preference is given to the use of the Gibbs free energy of activation over the electronic, or potential, energy of activation as a basis for comparing alternative reaction pathways. The rate constant (k) for an elementary reaction step is defined in terms of the Gibbs activation barrier (ΔG_A) as

$$k = \kappa\left(\frac{k_B T}{h}\right)\exp\left(\frac{-\Delta G_A}{RT}\right) = \kappa\left(\frac{k_B T}{H}\right)\exp\left(\frac{\Delta S_A}{R}\right)\exp\left(\frac{-\Delta H_A}{RT}\right)$$

where κ is the transmission coefficient, k_B is the Boltzmann constant, and ΔS_A and ΔH_A are the entropic and enthalpic activation barriers, respectively. By incorporating entropy effects, the Gibbs activation barrier provides a more complete representation of intrinsic reaction kinetics at nonzero temperatures than the electronic activation barrier.

The two chief sources of potential nonsystematic error for calculations with the $Ti(OH)_3(OOH)$ cluster models are the lack of steric constraints and alterations in the electronic properties of the titanium center and neighboring oxygen atoms caused by cluster truncation. These issues have been addressed for several of the trends reported here using constrained $Ti(OSiH_3)_3(OOH)$ clusters representing the second coordination sphere of the titanium active site. The construction of the $Ti(OSiH_3)_3(OOH)$ cluster model is described in our previous study.[10] The silicon atoms in this model were fixed, and the resulting constrained cluster was used as the starting point for all calculations involving the larger model. These clusters will be labeled as $Ti(OSiH_3)_3(OOH)(\eta^1$ or $\eta^2)-(\nu$S[O#], ROH[HB-α or HB-β]) using the nomenclature described previously.

Results and Discussion

Epoxidation Mechanism. Following the suggestions of previous investigators, an oxygen-transfer mechanism was considered in which ethylene attacks the proximal oxygen (Oα) of the hydroperoxo group in a spiro orientation to the plane containing the titanium atom and the hydroperoxo oxygens. Transition-state searches were also attempted using an initial planar orientation of ethylene with respect to the TiOO plane, but the ethylene molecule invariably optimized into a spiro orientation. Attack of the distal oxygen (Oβ) was not considered to any significant extent because previous studies[15,17−18] and our own exploratory calculations have shown proximal attack to be significantly more favored. Yudanov et al.[18] investigated a distal attack mechanism which involved the concerted cleavage of the Oα−Oβ bond and transfer of the proton from Oβ to Oα. The activation barrier for this distal attack mechanism exceeded the barrier for proximal attack by about 13 kcal/mol. Tantanak et al.[17] considered an alternative distal attack mechanism in which the proton on Oβ is transferred to a hydroxyl oxygen, while the titanium center forms a double bond with Oα. They found that the activation barrier for this distal attack mechanism was over 20 kcal/mol greater than a proximal attack mechanism. We briefly considered a two-step distal attack mechanism for $TiOOH(\eta^2)-H_2O[O1]$ in which transfer of the Oβ−H unit to ethylene occurs first followed by proton transfer to Oα. Because the activation barrier for the first step of this distal attack mechanism was about 10 kcal/mol greater than the activation barrier for proximal attack, the distal attack mechanism was not considered further.

In agreement with the results of Sinclair and Catlow,[19] a stable optimized geometry for the coordination of ethylene directly to the titanium center could not be found. The adsorption of ethylene on the titanium hydroperoxo cluster is possible through a $\pi_{C=C} \rightarrow \sigma_{O-H}^*$ hydrogen-bonding interaction with either the hydroperoxo moiety or a protic ligand on titanium. The ethylene adsorption energy is about 2−2.5 kcal/mol for both cases. These hydrogen-bonding interactions must be broken, however, to permit attack of the proximal oxygen. Hence, ethylene adsorption does not occur as a step in the epoxidation mechanism.

Transition states for the epoxidation of ethylene have been calculated for titanium hydroperoxo complexes possessing a variety of aqueous coordination environments. The reactions and their resulting activation barriers are summarized in Table 1. Parts a−d of Figure 4 show representative reaction pathways for ethylene epoxidation with titanium hydroperoxo intermediates bearing (a) no ligands, (b) one water ligand, (c) two water ligands, and (d) one water ligand and one protic water molecule in the HB-α bridging position.

The relative stabilities and important structural features of the titanium hydroperoxo reactant clusters in Table 1 have been considered at length in our earlier report.[10] Addition of a single water ligand to the titanium center in $Ti(OH)_3(OOH)$ yields a

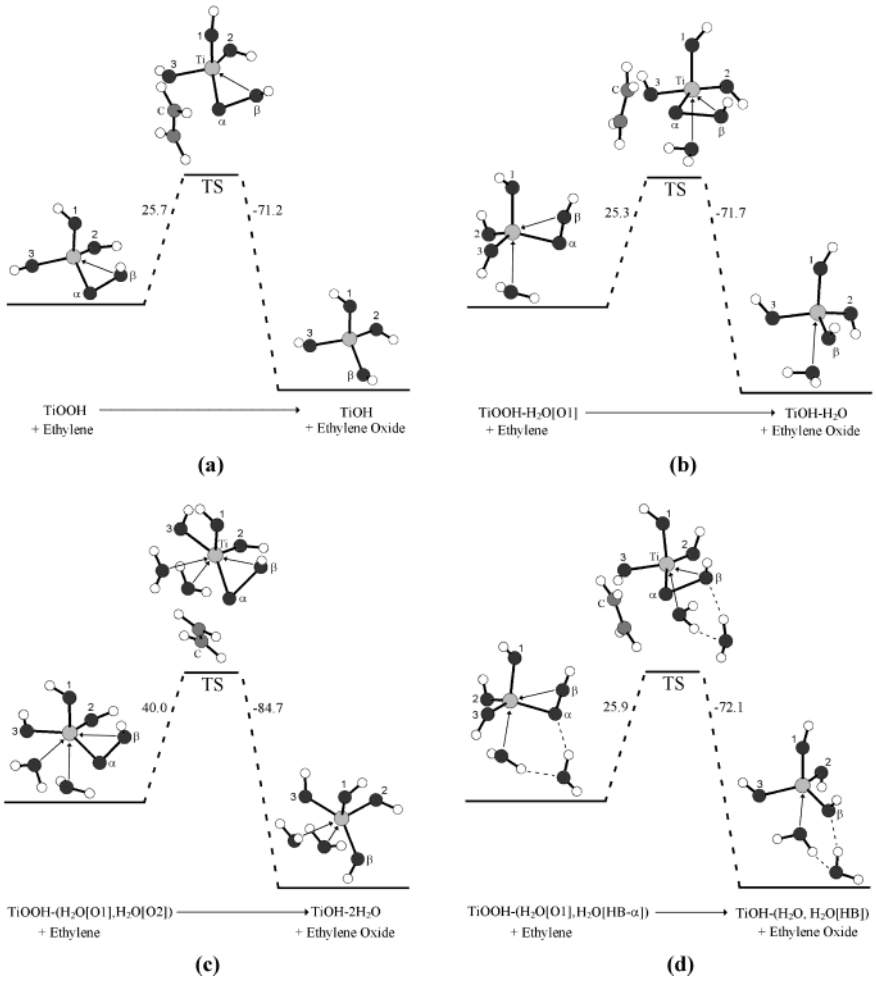

Figure 4. Representative reaction pathways for ethylene epoxidation with titanium hydroperoxo intermediates bearing (a) no ligands, (b) one water ligand, (c) two water ligands, and (d) one water ligand and one protic water molecule in the HB-α bridging position. The structures of the ethylene reactant and the ethylene oxide product have been omitted for the stable states. The oxygen labeling scheme used for the titanium hydroperoxo cluster has been extrapolated to the product and transition state clusters. Gibbs free energy changes are calculated in kcal/mol for all species at infinite separation.

multiplicity of degenerate $TiOOH-H_2O$ structures with an endothermic Gibbs free energy change of about 5−6 kcal/mol. When a water ligand coordinates the $Ti(OH)_3(OOH)$ cluster trans to hydroxyl oxygen O1 or O2, the hydroperoxo moiety may assume monodentate or bidentate coordination with the titanium center. The monodentate $TiOOH(\eta^1)-H_2O[O1]$ and $TiOOH(\eta^1)-H_2O[O2]$ structures are equivalent and will be labeled $TiOOH(\eta^1)-H_2O[O1/O2]$; the bidentate structures will be labeled $TiOOH(\eta^2)-H_2O[O1]$ and $TiOOH(\eta^2)-H_2O[O2]$. In the case of $TiOOH(\eta^1)-H_2O[O1/O2]$, monodentate coordination is stabilized by a hydrogen bond between the hydroperoxo group and a hydroxyl oxygen as shown in the optimized structure in Figure 5a. The hydroperoxo moiety in $TiOOH(\eta^1)-H_2O[O3]$ is stabilized in monodentate coordination with titanium through a hydrogen bond between the water ligand and the distal oxygen of the hydroperoxo group. The optimized geometry for $TiOOH(\eta^1)-H_2O[O3]$ is shown in Figure 5b. This structure resembles the hydrogen-bonded five-membered ring titanium hydroperoxo species proposed by Clerici and co-workers[2,11] (Figure 2) as the active oxygen-donating intermediate for epoxidation reactions performed in protic media with titanium-containing molecular sieves. It should be noted that the hydrogen-bonding motif observed in the structure of $TiOOH-(\eta^1)-H_2O[O1/O2]$ (Figure 5a) also constitutes a five-membered ring. To avoid ambiguous nomenclature, only the cyclic hydrogen-bonding motif proposed by Clerici and co-workers

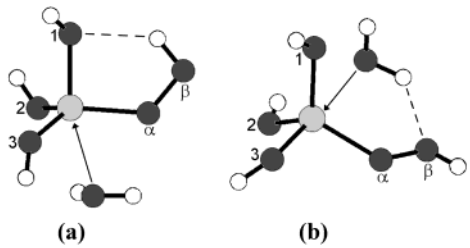

Figure 5. Stabilization of monodentate coordination by (a) hydrogen bonding between the hydrogen of the hydroperoxo group and a hydroxyl oxygen in $TiOOH(\eta^1)-H_2O[O1/O2]$ or (b) hydrogen bonding between the distal oxygen of the hydroperoxo group and a protic ligand on titanium in $TiOOH(\eta^1)-H_2O[O3]$.

where the coordinated solvent ligand directly participates in the ring will be referred to as the "five-membered ring intermediate" in the remainder of this discussion. The Gibbs free energy change for addition of a protic water molecule in the HB-α or HB-β bridging positions is small (endothermic or exothermic by less than 1 kcal/mol). The $TiOOH-H_2O$ and $TiOOH-(H_2O,$ H_2O[HB-α or HB-β]) clusters therefore possess similar relative stabilities. For the cases considered here, the hydroperoxo group invariably assumes bidentate coordination when interacting with a hydrogen-bonded bridging protic molecule. On the basis of thermodynamic and kinetic calculations, $TiOOH-H_2O$ and $TiOOH-(H_2O,$ H_2O[HB-α or HB-β]) species are predicted to

TABLE 2: Important Bond Distances for the Ethylene Epoxidation Transition-State Clusters[a]

	D(Oα−Oβ)		D(Ti−Oα)		D(Ti−Oβ)	
transition-state cluster	TS	change	TS	change	TS	change
TS−TiOOH(η^2)	1.779	0.317	1.941	0.068	2.067	−0.218
TS−TiOOH(η^1)−H_2O[O1/O2]	1.779	0.346	1.999	0.135	2.056	−0.836
TS−TiOOH(η^2)−H_2O[O1]	1.779	0.319	1.999	0.109	2.056	−0.324
TS−TiOOH(η^2)−H_2O[O2]	1.775	0.320	1.974	0.080	2.092	−0.330
TS−TiOOH(η^1)−H_2O[O3]	1.779	0.337	1.998	0.108	2.056	−0.878
TS−TiOOH(η^2)−(H_2O[O1], H_2O[O2])	1.821	0.361	2.034	0.108	2.038	−0.344
TS−TiOOH(η^1)−(H_2O[Oα], H_2O[O2])	1.805	0.379	2.015	0.181	2.039	−0.805
TS−TiOOH(η^2)−(H_2O[O1], H_2O[HB-α])	1.769	0.310	2.006	0.088	2.115	−0.317
TS−TiOOH(η^2)−(H_2O[O1], H_2O[HB-β])	1.769	0.304	2.006	0.094	2.115	−0.337
TS−TiOOH(η^2)−(H_2O[O1], H_2O[O2], H_2O[HB-α])	1.774	0.322	2.074	0.118	2.131	−0.302
TS−Ti$(OSiH_3)_3$(OOH)(η^2)	1.797	0.332	1.966	0.088	2.043	−0.249
TS−Ti$(OSiH_3)_3$(OOH)(η^2)−H_2O[O1]	1.781	0.313	2.013	0.092	2.076	−0.216
TS−Ti$(OSiH_3)_3$(OOH)(η^1)−H_2O[O3]	1.781	0.337	2.013	0.109	2.076	−0.878

[a] Bond distances in Å with changes calculated relative to the reactant cluster.

be the most abundant titanium hydroperoxo intermediates.[10] The addition of a second water ligand to titanium produces an endothermic Gibbs free energy change of about 6−7 kcal/mol. The resulting TiOOH−$2H_2O$ species may assume a variety of degenerate monodentate or bidentate structures depending upon the orientation of the ligands with respect to the hydroperoxo moiety. TiOOH−$2H_2O$ intermediates are not expected to be present in large amounts.

NBO analysis reveals that the primary donor−acceptor interaction arising from solvent ligand coordination at the Ti$(OH)_3$(OOH) cluster is a donation from a lone pair on the solvent ligand to the σ_{Ti-O}* antibonding orbital positioned directly across from it. This pattern of $n_S \rightarrow \sigma_{Ti-O}$* delocalization indicates the existence of a near-linear 3-center, 4-electron hypervalent ω bond between the solvent ligand, the titanium center, and the oxygen atom positioned trans to the ligand. The important electronic properties of these solvent ligand ω bonds have been extensively discussed in our previous report.[10] The principal donor−acceptor interaction stabilizing the bidentate coordination of the distal hydroperoxo oxygen Oβ is another ω bond between a lone pair on Oβ and the σ_{Ti-O3}* antibonding orbital.

Important bond lengths of the epoxidation transition states are listed in Table 2. In accordance with earlier reports, ethylene epoxidation follows an electrophilic mechanism in which the $\pi_{C=C}$ bond of the alkene transfers electrons into the σ_{O-O}* peroxo antibond of the titanium hydroperoxo intermediate. Second-order perturbation theory estimates of the electron-transfer accompanying the $\pi_{C=C} \rightarrow \sigma_{O-O}$* donor−acceptor interaction range between 1.0 and 1.3 electrons for the reactions listed in Table 1. This electron donation dramatically elongates the O−O bond and eventually leads to its cleavage (Table 2). In addition to breaking the O−O bond, transfer of the proximal oxygen Oα to the alkene substrate also requires cleavage of the Ti−Oα bond and formation of a Ti−Oβ bond. As a result, the Ti−Oα distance increases in the transition state, whereas the Ti−Oβ distance decreases. In the optimized transition-state geometries, the Ti−Oα and Ti−Oβ distances are similar.

Particularly interesting are the structural changes that occur in clusters TiOOH(η^1)−H_2O[O1/O2] and TiOOH(η^1)−H_2O[O3] as they react with ethylene. The strong electron donation from ethylene into the σ_{O-O}* antibond and the concomitant increase in O−O bond length disrupts the relatively weak hydrogen bond in TiOOH(η^1)−H_2O[O1/O2] and TiOOH(η^1)−H_2O[O3], and the hydroperoxo group assumes bidentate coordination with titanium in the transition states for both species. Bidentate coordination of the hydroperoxo moiety in the transition state is once again stabilized through a $n_{O\beta} \rightarrow \sigma_{Ti-O3}$* donor−acceptor interaction. The final TS−TiOOH(η^1)−H_2O[O1/O2] and TS−TiOOH(η^1)−H_2O[O3] transition states closely resemble the TS−TiOOH(η^2)−H_2O[O1] transition state. The same phenomenon is observed for epoxidation with the constrained, five-membered ring Ti$(OSiH_3)_3$(OOH)(η^1)−H_2O[O3] intermediate. Electron donation from the $\pi_{C=C}$ bond of ethylene into the σ_{O-O}* antibond of Ti$(OSiH_3)_3$(OOH)(η^1)−H_2O[O3] disrupts the hydrogen bond between the water ligand and the hydroperoxo group, thereby allowing the hydroperoxo group to assume bidentate coordination in the transition state.

In the case of the nonligated TiOOH(η^2) intermediate, the electronic (ΔE_A) and Gibbs (ΔG_A) activation barriers for ethylene epoxidation are 14.8 and 25.7 kcal/mol, respectively (Table 1). These activation barriers are calculated as the difference between the energy of the transition state and the energies of ethylene and the titanium hydroperoxo cluster at infinite separation. The Gibbs activation barrier is higher than the electronic activation barrier because of the entropy loss associated with binding the ethylene substrate to the titanium hydroperoxo oxidant in the transition-state complex. The entropic contribution raises the Gibbs activation barrier for the TiOOH(η^2) cluster by 11.4 kcal/mol at 298 K. An entropy loss of similar magnitude ($T\Delta S_A = -11$ to -13 kcal/mol) increases the Gibbs activation barrier for each titanium hydroperoxo cluster considered in this study (Table 1). For the remainder of this discussion, the term "activation barrier" will refer to the Gibbs activation barrier unless stated otherwise.

As discussed in our previous study,[10] the titanium hydroperoxo intermediate is formed by proton transfer from a hydrogen peroxide ligand to a hydroxyl oxygen atom. For the Ti$(OH)_3$(OOH) cluster models considered in this study, the proton transfer step always generates a water ligand positioned trans to either hydroxyl oxygen O1 or O2. It should be noted, however, that the titanium center in an actual titanium-based epoxidation catalyst generally possesses two, three, or four Ti−O−Si bonds to the siliceous framework or support. Hence, proton transfer from a hydrogen peroxide ligand to a framework oxygen may lead to the formation of a silanol group coordinating the titanium center rather than a water ligand. Many of the trends discussed here should be relevant for ethylene epoxidation with both silanol-coordinated and water-coordinated titanium hydroperoxo intermediates, but the absolute magnitudes of the energy differences are expected to more accurately represent the latter case.

The epoxidation activation barriers for the TiOOH(η^1)−H_2O[O1/O2], TiOOH(η^2)−H_2O[O1], and TiOOH(η^2)−H_2O[O2] clusters are 24.8, 25.3, and 24.2 kcal/mol, respectively. The hydroperoxo moiety in these clusters may reorient to yield the

TABLE 3: Effects of Ligand Location, Ligand Identity, and Peroxide Identity on Structural Properties of the Peroxo Group and Activation Barriers for Ethylene Epoxidation

						thermochemistry at 298 K		
$Ti(OH)_3(OOR)$ cluster	ΔE_{ads}[a]	$D(O\alpha-O\beta)$[b]	$D(Ti-O\alpha)$	$D(Ti-O\beta)$	ΔE_A[c]	ΔH_A	$T\Delta S_A$	ΔG_A
$TiOOH(\eta^2)$	0	1.462	1.873	2.285	14.8	14.3	−11.4	25.7
$TiOOH(\eta^2)-H_2O$[O1]	−4.3	1.460	1.892	2.380	14.5	14.0	−11.4	25.3
$TiOOH(\eta^2)-$MeOH[O1]	−5.4	1.460	1.888	2.372	15.5	15.1	−11.4	26.5
$TiOOH(\eta^2)-NH_3$[O1]	−6.3	1.462	1.912	2.345	15.0	14.4	−11.7	26.1
$TiOOH(\eta^2)-CH_3CN$[O1]	1.5	1.458	1.884	2.357	13.2	13.3	−9.2	22.5
$TiOOH(\eta^2)-H_2O$[Oα]	−3.1	1.458	1.867	2.400	20.8	19.8	−12.5	32.3
$TiOOH(\eta^2)-$MeOH[Oα]	−3.4	1.458	1.866	2.387	18.5	21.1	−11.5	32.6
$TiOOH(\eta^2)-NH_3$[Oα]	−8.0	1.460	1.899	2.231	22.0	21.3	−11.7	33.1
$TiOOH(\eta^2)-CH_3CN$[Oα]	−0.3	1.460	1.869	2.360				
$TiOOCH_3(\eta^2)$		1.461	1.870	2.287	18.0	17.4	−10.9	28.3
$TiOOCF_3(\eta^1)$		1.447	1.889	2.697	10.6	10.1	−11.8	21.9

[a] Ligand adsorption energy in kcal/mol. [b] Bond distances in Å. [c] Activation barriers in kcal/mol.

five-membered ring intermediate, $TiOOH(\eta^1)-H_2O$[O3]. The activation barrier for ethylene epoxidation with $TiOOH(\eta^1)-H_2O$[O3] is 25.2 kcal/mol. Thus, hydrogen bonding with a protic solvent ligand via a five-membered ring does not significantly alter the reactivity of the titanium hydroperoxo intermediate in ethylene epoxidation. The possible existence of five-membered ring intermediates therefore does not explain the epoxidation rate enhancement observed experimentally in protic solvents. Comparison of the results for the nonligated $TiOOH(\eta^2)$ cluster and the mono-ligated $TiOOH-H_2O$ clusters indicates that the presence of the single water ligand generated during titanium hydroperoxo intermediate formation has little effect on epoxidation reactivity. The use of larger, constrained $Ti(OSiH_3)_3(OOH)$ cluster models does not alter these reactivity trends. The activation barriers for $Ti(OSiH_3)_3(OOH)(\eta^2)$, $Ti(OSiH_3)_3(OOH)(\eta^2)-H_2O$[O1], and $Ti(OSiH_3)_3(OOH)(\eta^1)-H_2O$[O3] are 25.9, 24.9, and 25.1 kcal/mol, respectively.

Coordination of a second water ligand at the titanium center strongly deactivates the titanium hydroperoxo intermediate for ethylene epoxidation. The activation barriers for $TiOOH(\eta^2)-(H_2O$[O1], H_2O[O2]) and $TiOOH(\eta^1)-(H_2O$[Oα], H_2O[O2]) are 40.0 and 36.4 kcal/mol, respectively. Figure 4c shows the epoxidation pathway for the $TiOOH(\eta^2)-(H_2O$[O1], H_2O[O2]) case. The water ligands sterically hinder the attack of the ethylene substrate at the proximal hydroperoxo oxygen. Substantial structural deformation must occur in order to allow attack of the proximal oxygen, and this deformation raises the energy of the transition state and the activation barrier.

The results in Table 1 show that the presence of a protic water molecule in either the HB-α or HB-β bridging position of the titanium hydroperoxo intermediate has little effect on the activation barrier for ethylene epoxidation. The epoxidation reactions for $TiOOH(\eta^2)-(H_2O$[O1], H_2O[HB-α]) and $TiOOH(\eta^2)-(H_2O$[O1], H_2O[HB-β]) pass through the same transition state (shown in Figure 4d). In that transition state, the protic water molecule donates a hydrogen bond to the distal hydroperoxo oxygen instead of the proximal oxygen in order to accommodate transfer of the proximal oxygen to the ethylene substrate. The activation barriers for $TiOOH(\eta^2)-(H_2O$[O1], H_2O[HB-α]) and $TiOOH(\eta^2)-(H_2O$[O1], H_2O[HB-β]) are 25.9 and 25.2 kcal/mol, respectively. An activation barrier of 37.3 kcal/mol was calculated for ethylene epoxidation with the $TiOOH(\eta^2)-(H_2O$[O1], H_2O[O2], H_2O[HB-α]) cluster. This high activation barrier can once again be attributed to the steric hindrance caused by the two water ligands on the titanium center.

Because these epoxidation reactions are typically performed under liquid-phase reaction conditions within the pores of a titanosilicate material, we have attempted to estimate the possible effect of a polarizable reaction medium on the activation barriers reported in Table 2. We used the IEF−PCM method with methanol as solvent ($\epsilon = 32.63$) in order to provide a highly polarizable reaction medium. The Gibbs activation barriers for TiOOH, $TiOOH-H_2O$[O1], and $TiOOH-(H_2O$[O1], H_2O[HB-α]) are all significantly increased to 28.5, 27.8, and 28.2 kcal/mol, respectively. These calculated increases in the activation barrier due to an induced electric field are in accordance with the recent computational results of Truong and co-workers,[27] which showed that the Madelung electric field raises the activation barrier for ethylene epoxidation with titanium silicalite-1 catalyst. The important conclusion is that the presence of a polarizable reaction medium uniformly alters the activation barriers and does not change the reactivity trends discussed above.

Ligand Exchange Effects. It has been shown that the presence of the single water ligand generated during titanium hydroperoxo intermediate formation does not significantly affect the activation barrier for ethylene epoxidation. It is possible under liquid-phase reaction conditions that this water ligand may exchange with other solvent ligands. As a result of ligand exchange, it is also possible that a water or other donor ligand may coordinate the titanium center in a position trans to the proximal oxygen (Oα) of the hydroperoxo group. To assess the effects of ligand exchange, we have optimized transition states for ethylene epoxidation with titanium hydroperoxo intermediates bearing a single water, methanol, ammonia, or acetonitrile ligand oriented trans to either hydroperoxo oxygen Oα or hydroxyl oxygen O1. Methanol and acetonitrile are both common solvents for the $Ti(IV)-H_2O_2$ catalytic system; ammonia was chosen as a model ligand only to allow comparison with the previous study by Yudanov et al.[18] The results are summarized in Table 3.

It is apparent that the identity of the solvent ligand makes little difference when that ligand is located across from hydroxyl oxygen O1. The activation barrier for the $TiOOH(\eta^2)-CH_3CN$[O1] cluster is slightly lower than the other $TiOOH(\eta^2)-S$[O1] clusters because the weakly bound acetonitrile ligand is partially expelled from the titanium coordination sphere during the epoxidation reaction, resulting in an entropy gain and a decrease in the Gibbs activation barrier. By analogy with the results described above for coordination of a single water ligand, it is expected that solvent ligand identity also will not matter for coordination positions O2 or O3. When one ligand coordinates the titanium cluster in an orientation that permits formation of a hypervalent ω bond with the proximal oxygen atom of the hydroperoxo group, however, the activation barrier for ethylene

TABLE 4: Natural Population and Natural Bond Orbital[a] Analysis of $Ti(OH)_3(OOR)$ Complexes (R = H, CH_3, or CF_3)

$Ti(OH)_3(OOR)$ cluster	charge on Oα	charge on Oβ	total O−O charge	charge on Ti	charge on H/C[b]	σ_{O-O}* population	σ_{O-O}* energy	$\sigma_{Ti-O\alpha}$ population	$\sigma_{Ti-O\alpha}$ C_{Ti}[c]	$\sigma_{Ti-O\alpha}$ Ti hybrid
$TiOOH(\eta^2)$	−0.440	−0.454	−0.893	1.716	0.482	0.00441	0.0442	1.9509	0.3570	$sd^{4.9}$
$TiOOH(\eta^2)-H_2O[O\alpha]$	−0.429	-0.453	−0.881	1.676	0.477	0.00608	0.0615	1.9774	0.3794	$sd^{2.0}$
$TiOOH(\eta^1)-H_2O[O1/O2]$	−0.501	-0.416	−0.918	1.661	0.466	0.01635	0.1013	1.9851	0.3753	$sd^{4.8}$
$TiOOH(\eta^2)-H_2O[O1]$	−0.477	-0.447	−0.924	1.672	0.477	0.00471	0.0601	1.9147	0.3208	$sd^{4.3}$
$TiOOH(\eta^2)-H_2O[O2]$	−0.481	−0.447	−0.928	1.670	0.473	0.00701	0.0637	1.9479	0.3464	$sd^{5.3}$
$TiOOH(\eta^1)-H_2O[O3]$	−0.491	−0.488	−0.979	1.697	0.478	0.00931	0.0839	1.9231	0.2980	$sd^{3.6}$
$TiOOH(\eta^2)-MeOH[O\alpha]$	−0.427	−0.451	−0.878	1.683	0.478	0.00591	0.0605	1.9733	0.3786	$sd^{2.0}$
$TiOOH(\eta^2)-MeOH[O1]$	−0.466	−0.447	−0.913	1.672	0.477	0.00412	0.0669	1.9495	0.3550	$sd^{3.8}$
$TiOOH(\eta^2)-NH_3[O\alpha]$	−0.432	−0.447	−0.879	1.610	0.487	0.04335	0.0513	1.9690	0.3682	$sd^{2.0}$
$TiOOH(\eta^2)-NH_3[O1]$	−0.466	−0.466	−0.932	1.616	0.480	0.00332	0.0716	1.9295	0.3222	$sd^{7.1}$
$TiOOH(\eta^2)-CH_3CN[O\alpha]$	−0.420	−0.453	−0.874	1.645	0.481	0.00734	0.0731	1.9776	0.3826	$sd^{2.0}$
$TiOOH(\eta^2)-CH_3CN[O1]$	−0.450	−0.445	−0.895	1.646	0.478	0.00385	0.0782	1.9881	0.3814	$sd^{4.9}$
$TiOOCH_3(\eta^2)$	−0.440	−0.337	−0.777	1.721	−0.207	0.02445	0.0502	1.9806	0.3801	$sd^{3.7}$
$TiOOCF_3(\eta^1)$	−0.460	−0.325	−0.785	1.768	1.275	0.02051	0.0465	1.9164	0.3136	$sd^{3.1}$

[a] Results obtained for single optimized NBO representations of the clusters that possess identical peroxo bond Lewis structures: single bonds for Ti−Oα, Ti−Oβ, and O−O and two lone pairs on both Oα and Oβ. [b] Charge on the hydrogen or carbon atom bonded to the distal hydroperoxo oxygen. [c] Polarization coefficient for the titanium atom in the $\sigma_{Ti-O\alpha}$ bond.

epoxidation increases by about 6−7 kcal/mol. The order of the increase in the electronic activation barrier, ΔE_A, is in accordance with the expected donor properties of the ligands: methanol < water < ammonia. An activation barrier for the $TiOOH(\eta^2)-CH_3CN[O\alpha]$ case could not be calculated because the weakly bound acetonitrile ligand was completely expelled from the coordination sphere of titanium during the reaction.

As mentioned earlier, the primary processes taking place during the epoxidation reaction are the heterolytic cleavage of the O−O and Ti−Oα bonds and the formation of a Ti−Oβ bond. An increase in the activation barrier of the reaction most likely reflects increased difficulty in performing some subset of these three steps. The effects of ligand position on these processes are considered below.

Because the most dramatic change in the transition state is the elongation of the peroxo bond, it is perhaps natural to assume that ligand coordination trans to the proximal hydroperoxo oxygen deactivates the cluster for oxygen transfer by either strengthening the peroxo bond or reducing its electrophilicity. One measure of peroxo bond strength is the O−O bond distance. Table 3 shows that the O−O bond length is not significantly smaller when a solvent ligand coordinates titanium trans to the proximal hydroperoxo oxygen than when a solvent ligand coordinates titanium trans to hydroxyl oxygen O1. In addition, NBO analysis indicates that coordination of a single ligand does not produce any notable changes in the polarization or hybridization of the peroxo bond (results not shown). Hence, ligand coordination across from the proximal oxygen does not appear to deactivate transfer of the proximal oxygen by strengthening the peroxo bond.

Increases in the total charge on the peroxo group, the charge on the attacked proximal oxygen, and the energy of the σ_{O-O}* antibond are all expected to decrease the electrophilicity of the peroxo group. These important characteristics of the peroxo group are listed for the mono-ligated titanium hydroperoxo clusters in Table 4. When a single solvent molecule coordinates the titanium center, the negative charge on the proximal oxygen decreases if the ligand is positioned across from Oα and increases if the ligand is positioned elsewhere. The origin of this trend is difficult to clearly discern because the vacant *d*-shell hypovalency of the titanium center requires a complicated, multiresonance NBO representation for the titanium hydroperoxo cluster. A decrease in the negative charge on Oα when it participates in an $\omega_{Ti-O\alpha}$ bond can likely be traced to the decreased polarization of the $\omega_{Ti-O\alpha}$ bond compared to the $\sigma_{Ti-O\alpha}$ bond. The total negative charge on the peroxo group is also lower in the case of ligand coordination across from the proximal oxygen. No definitive trends can be observed in the energy of the σ_{O-O}* antibonding orbital with respect to varying ligand position. These results suggest that the electrophilicity of the peroxo group in the TiOOH−S[Oα] clusters is not less than in the other monoligated clusters.

Thus, one can conclude that the changes in the properties of the peroxo group caused by varying the location of the solvent ligand do not affect the activation barrier for the epoxidation reaction. This conclusion can be extended to suggest that changes in the properties of the peroxo group caused by the addition of a single donor ligand at any position do not affect the activation barrier. This latter conclusion is supported by the observation that coordination of water at positions trans to hydroxyl oxygens O1, O2, and O3 noticeably reduces the electrophilicity of the peroxo group (by increasing the charge on Oα, the total O−O charge, and the σ_{O-O}* antibonding energy), yet the activation barrier for the electrophilic epoxidation reaction does not change appreciably. The strong donation of electrons from the $\pi_{C=C}$ bond of ethylene into the σ_{O-O}* antibond of the titanium hydroperoxo cluster appears to occur readily despite substantial changes in the electrophilicity of the peroxo group.

The existence of a strong $n_S \rightarrow \sigma_{Ti-O\alpha}$* ω-bond interaction in the case of the TiOOH−S[Oα] clusters and its absence in the other monoligated clusters strongly suggests that the activation barrier for ethylene epoxidation increases because this donor−acceptor interaction inhibits heterolytic cleavage of the Ti−Oα bond. Upon initial inspection, this claim does not seem plausible because donation into an antibonding orbital should elongate and weaken the corresponding bond. The Ti−Oα bond length in the $TiOOH(\eta^2)-NH_3[O\alpha]$ cluster is indeed slightly longer than in the nonligated $TiOOH(\eta^2)$ cluster, but the Ti−Oα bond lengths in the other TiOOH−S[Oα] clusters are actually slightly shorter despite the strong electron donation into the $\sigma_{Ti-O\alpha}$* antibond (Table 3). To understand these results, it should be recalled[10] that ω-bond formation also entails rehybridization of the titanium hybrid in the Ti−Oα bond from sd^{4-7} to sd^2. The increased s character of the titanium hybrid tends to reduce the length of the Ti−Oα bond. In the $TiOOH(\eta^2)-NH_3[O\alpha]$ cluster, the Ti−Oα bond elongation caused by the strong electron donation from the ligand into the $\sigma_{Ti-O\alpha}$* antibond outweighs the bond shortening caused by the rehybridization. In the other TiOOH−S[Oα] clusters, however, the

$n_S \rightarrow \sigma_{Ti-O\alpha}$* donor−acceptor interactions are weaker, leading to an overall decrease in Ti−Oα bond length. In all cases, the rehybridization of the Ti−Oα bond increases the probability of finding the bond electrons closer to the titanium atom. As a result, it becomes more difficult for the electrons to join the epoxide product via heterolytic cleavage of the Ti−Oα bond. The activation barrier for the transfer of the proximal hydroperoxo oxygen should therefore increase when that oxygen forms an ω bond with a solvent ligand.

It is difficult to ascertain any effect of ligand position on formation of the Ti−Oβ bond during ethylene epoxidation. Formation of the Ti−Oβ bond is primarily controlled by the strong donation of electrons from the ethylene $\pi_{C=C}$ into the σ_{O-O}* antibond and the dramatic electronic and structural alterations it engenders in the peroxo group. Compared to this interaction, the electronic effects of ligand coordination on the distal hydroperoxo oxygen are relatively weak. The ligand may have a steric effect on formation of the Ti−Oβ bond through occupation of potential coordination sites. Inspection of the optimized transition state geometries for the monoligated clusters suggests, however, that such steric effects are probably minor for the cluster models considered here.

Comparison with Previous Studies. The electronic activation barriers, ΔE_A, for ethylene epoxidation obtained in this investigation are similar in magnitude to ones reported in previous computational studies. Sinclair and Catlow[19] have calculated an electronic activation barrier of 10.3 kcal/mol for the oxygen transfer step in the epoxidation of ethylene with a nonligated, constrained $Ti(OH)(OSiH_3)_2(OOH)$ cluster using a BP86/DZVP approach. It is generally found that pure density functionals, such as BP86, tend to yield lower activation barriers than hybrid density functionals, such as B3LYP, because hybrid functionals partially account for exact exchange.[28,29] Reoptimization of our TiOOH(η^2) and TS−TiOOH(η^2) clusters using BP86 with the original basis set yield an electronic activation barrier of 7.5 kcal/mol. The use of an effective core potential to model titanium has little effect upon the activation barriers. The electronic and Gibbs activation barriers for ethylene epoxidation with TiOOH(η^2) become 14.6 and 25.1 kcal/mol, respectively, upon reoptimization with an all electron B3LYP/6-311+G(d,p) methodology. Using a computational strategy similar to the one employed here, Yudanov et al.[18] have calculated electronic activation barriers of 12.7 and 12.4 kcal/mol for the epoxidation of ethylene with the model titanium hydroperoxo clusters TiOOH(η^2) and TiOOH(η^2)−NH_3[O1], respectively. Their results support the hypothesis advanced here that coordination of a single ligand trans to the hydroxyl oxygens (as opposed to coordination of a single ligand trans to the proximal hydroperoxo oxygen) has little effect on the reactivity of the titanium hydroperoxo intermediate in epoxidation reactions. Using a B3LYP/3-21G(d) approach, Tantanak et al.[17] calculated an 11.9 kcal/mol electronic activation barrier for ethylene epoxidation with an unconstrained $Ti(OSiH_3)_3(OOH)\cdot$MeOH cluster which corresponds to our TiOOH−MeOH[O1] case. Munakata et al.[20] calculated an electronic activation barrier of 18.4 kcal/mol for transfer of the proximal oxygen in a $Ti[OSi(OH)_3]_3[OOSi(OH)_3]$ species with a water ligand positioned trans to a siloxyl oxygen. None of these researchers have reported thermochemistry results for these reactions. No other activation barriers have been reported for titanium hydroperoxo clusters that include donor ligands on titanium or hydrogen-bonded solvent molecules.

DFT calculations typically underestimate actual activation barriers. Few experimentally measured activation barriers for comparable alkene epoxidation reactions are available. The apparent activation energy for 1-hexene epoxidation with hydrogen peroxide using a TS-1 catalyst has been reported[6] to be 15.5 ± 1.5 kcal/mol in MeOH, a value very similar to the ΔH_A values calculated in this study.

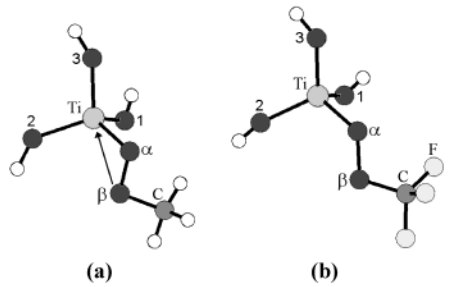

Figure 6. Optimized geometries for (a) $TiOOCH_3(\eta^2)$ and (b) $TiOOCF_3(\eta^1)$.

Other Oxidants. The optimized geometries for the $Ti(OH)_3(OOCH_3)$ and $Ti(OH)_3(OOCF_3)$ clusters are shown in parts a and b of Figure 6, respectively, and their important peroxo group structural parameters are listed in Table 3. The methylperoxo and hydroperoxo clusters possess very similar geometries. Replacement of the methyl substituent with a trifluoromethyl substituent, however, leads to a slight decrease in the peroxo bond length and a transition from bidentate to monodentate coordination of the peroxo group.

The activation barriers for these two clusters are given in Table 3. In agreement with the results of Yudanov et al.,[18] the electronic activation barrier for the $TiOOCH_3(\eta^2)$ cluster exceeds the barrier for the TiOOH(η^2) cluster by about 3 kcal/mol. Yudanov et al. attributed this increase in ΔE_A to an electron-donating inductive effect of the methyl substituent that decreases the electrophilicity of the peroxo group. NBO analysis of the optimized $TiOOCH_3(\eta^2)$ cluster reveals, however, that the methyl group actually withdraws electrons from the distal oxygen Oβ and has essentially no effect on the charge of the proximal oxygen Oα (Table 4). In addition, the energy of the σ_{O-O}* antibond in the $TiOOCH_3(\eta^2)$ cluster is more positive than in the TiOOH(η^2) cluster but less positive than in the TiOOH(η^2)−H_2O[O1] cluster. Because TiOOH(η^2) and TiOOH(η^2)−H_2O[O1] have similar activation barriers, the increase in the σ_{O-O}* antibond energy cannot explain the deactivation of the $TiOOCH_3(\eta^2)$ cluster. Thus, the methyl substituent clearly does not reduce the reactivity of the $TiOOCH_3(\eta^2)$ cluster relative to the TiOOH(η^2) cluster by decreasing the electrophilicity of the peroxo group.

The results for the $TiOOCF_3(\eta^1)$ cluster provide a useful comparison. The electronic activation barrier for the $TiOOCF_3(\eta^1)$ cluster is about 4 kcal/mol less than the barrier for the TiOOH(η^2) cluster and about 7.5 kcal/mol less than the barrier for the $TiOOCH_3(\eta^2)$ cluster. Because the peroxo bond must be broken and a Ti−Oβ bond must be formed during ethylene epoxidation, one would expect that the structural changes introduced by the trifluoromethyl group would increase the activation barrier, not lower it. Comparison of the individual charges on the peroxo oxygens, total peroxo group charges, and σ_{O-O}* antibond energies for the $TiOOCF_3(\eta^1)$ and $TiOOCH_3(\eta^2)$ clusters indicates that the greater activity of the $TiOOCF_3(\eta^1)$ cluster also cannot be attributed to greater electrophilicity of the peroxo group.

These results may be understood by comparing the charge on the atom bonded to the distal peroxo oxygen for the titanium hydroperoxo, methylperoxo, and trifluoromethylperoxo clusters (Table 4). The carbon atoms in the $TiOOCH_3(\eta^2)$ and $TiOOCF_3$-

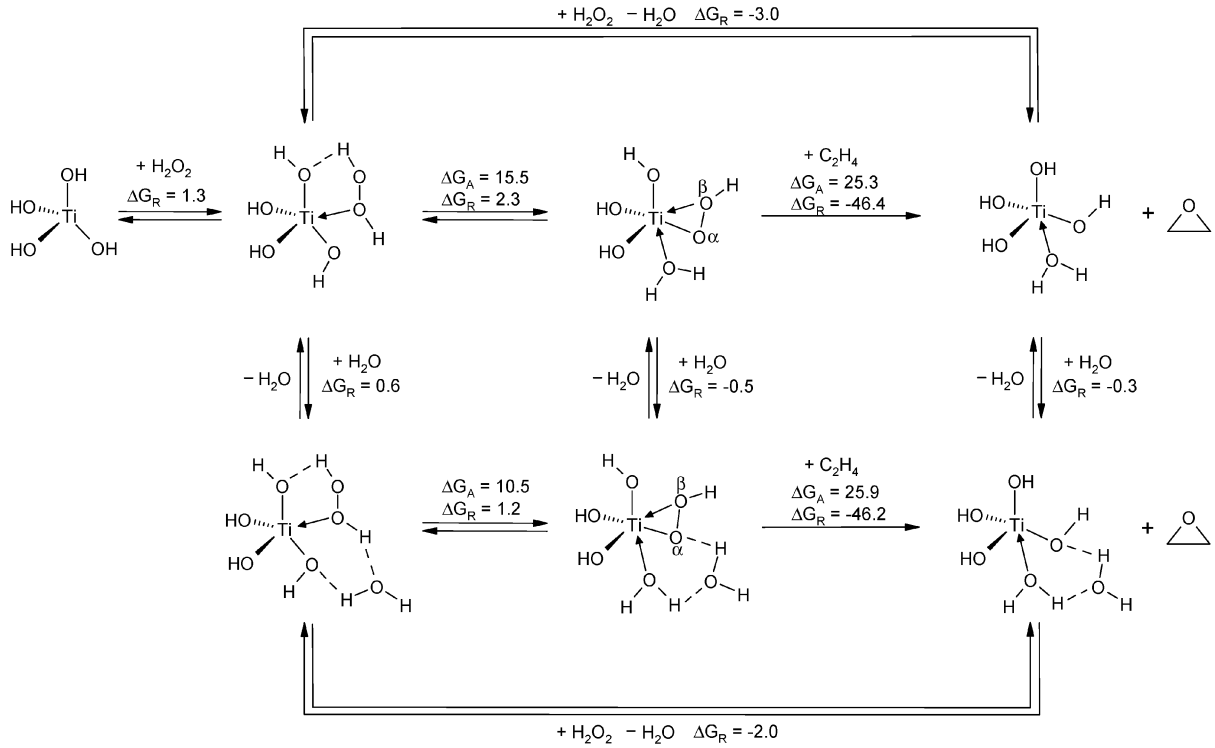

Figure 7. Reaction pathways for ethylene epoxidation with Ti(IV)−H_2O_2 in the presence of aqueous solvent coordination at the titanium active site. To simplify the reaction scheme, the many degenerate structures of the titanium hydroperoxo intermediate in the presence of solvent coordination and their associated degenerate epoxidation pathways have not been included. The activation barriers (ΔG_A) and reaction energies (ΔG_R) shown for the two reaction steps are taken from representative cases and are reported in kcal/mol.

(η^1) clusters withdraw more electrons from the distal peroxo oxygen than the less electronegative hydroperoxo proton in the titanium hydroperoxo clusters. In the $TiOOCH_3(\eta^2)$ case, the C−H bonds in the methyl substituent are polarized toward the carbon atom, and the carbon atom therefore acquires a more negative charge than the proton in the titanium hydroperoxo clusters. In the $TiOOCF_3(\eta^1)$ case, however, the C−F bonds are strongly polarized toward the fluorine atoms, and the carbon atom acquires a more positive charge than the proton in the titanium hydroperoxo clusters. During the epoxidation reaction, the distal peroxo oxygen receives additional electron density as the peroxo bond is cleaved. An increased positive charge on the atom bonded to the distal peroxo oxygen provides increased electrostatic stabilization of the negative charge developing on the distal hydroperoxo oxygen in the transition state. This increased stabilization decreases the energy of the transition state and the activation barrier for ethylene epoxidation.

Overall Catalytic Cycle. The two steps in the ethylene epoxidation mechanism are (1) formation of the titanium hydroperoxo intermediate and (2) transfer of the proximal hydroperoxo oxygen to the ethylene substrate. Our previous investigation[10] showed that the first step likely occurs with a Gibbs activation barrier between 9 and 16 kcal/mol and yields a titanium hydroperoxo intermediate bearing a single water ligand on titanium and possibly a protic molecule bridging that water ligand and a hydroperoxo oxygen via two hydrogen-bonding interactions. The presence of the water ligand or a bridging protic molecule has little effect on the Gibbs activation barrier for the oxygen transfer step compared to a nonligated titanium hydroperoxo intermediate. The activation barrier is approximately 24−26 kcal/mol for all such cases. Comparison of the Gibbs activation barriers for the two steps in the epoxidation mechanism indicates that the rate constant for intermediate formation should exceed the rate constant for oxygen transfer by at least 6 orders of magnitude. The oxygen transfer step is therefore the rate-determining step of the overall epoxidation mechanism.

The most probable reaction pathways for the epoxidation of ethylene with the Ti(IV)−H_2O_2 oxidation system under liquid-phase reaction conditions are summarized in Figure 7. The reaction pathways in Figure 7 are shown exclusively for the case of water coordination at the titanium site, but analogous pathways will exist for other protic solvents.

Conclusions

This report concludes our investigation of solvent coordination effects for the titanium-catalyzed epoxidation of ethylene with hydrogen peroxide as oxidant. Activation barriers have been calculated for oxygen transfer from titanium hydroperoxo complexes possessing a variety of coordination environments. In the case of monoligated complexes, the identity of the ligand and its orientation with respect to the hydroperoxo group have little effect on the activation barrier unless the ligand occupies a position that permits formation of an ω bond with the proximal oxygen of the hydroperoxo moiety. In that case, the ω bond inhibits the heterolytic cleavage of the Ti−Oα bond and increases the activation barrier by about 6−7 kcal/mol. The presence of two ligands on the titanium center is highly deactivating for all ligand orientations. The activation barrier is unaffected by the presence of a hydrogen-bonded protic solvent molecule bridging the hydroperoxo moiety and a protic ligand on titanium.

A protic solvent ligand on the titanium center may be oriented in such a way that a hydrogen-bonded five-membered ring species such as the one proposed by Clerici et al.[2,11] may be formed. We have shown here that hydrogen bonding with a protic solvent ligand in a five-membered ring does not augment the reactivity of the titanium hydroperoxo complex for ethylene epoxidation. Thus, the five-membered ring hypothesis cannot

be invoked as an explanation for the rate enhancement observed experimentally in protic solvents. Our results suggest that the origin of the rate enhancement does not arise from localized solvent coordination effects at the titanium active site. Instead, the solvent most likely affects reaction rates by controlling the intraporous concentration of alkene substrate and hydrogen peroxide oxidant available at the titanium active sites.

Examination of ethylene epoxidation kinetics with $Ti(OH)_3(OOCH_3)$ and $Ti(OH)_3(OOCF_3)$ intermediates indicates that other peroxide oxidants may demonstrate different intrinsic activities. NBO analysis of the electronic properties of various titanium peroxo (TiOOR) complexes reveals that their reactivity patterns cannot be explained solely by considering the electrophilicity of the peroxo group.

Acknowledgment. We gratefully acknowledge the financial support of the National Science Foundation Training Grant (DGE−9554586) for the program "Catalysis for Environmentally Conscious Manufacturing" and funding received through a National Science Foundation Fellowship (R.R.S.). We also thank Dr. Frank A. Weinhold for helpful discussions.

References and Notes

(1) Clerici, M. G.; Bellussi, G.; Romano, U. *J. Catal.* **1991**, *129*, 159−167.
(2) Clerici, M. G.; Ingallina, P. *J. Catal.* **1993**, *140*, 71−83.
(3) Sato, T.; Dakka, J.; Sheldon, R. A. *Stud. Surf. Sci. Catal.* **1994**, *84*, 1853−1860.
(4) Van der Waal, J. C.; van Bekkum, H. *J. Mol. Catal. A* **1997**, *124*, 137−146.
(5) Hulea, V.; Dumitriu, E.; Patcas, F.; Ropot, R.; Graffin, P.; Moreau, P. *Appl. Catal. A* **1998**, *170*, 169−175.
(6) Langhendries, G.; De Vos, D. E.; Baron, G. V.; Jacobs, P. A. *J. Catal.* **1999**, *187*, 453−463.
(7) Ingold, K. U.; Snelgrove, D. W.; MacFaul, P. A.; Oldroyd, R. D.; Thomas, J. M. *Catal. Lett.* **1997**, *48*, 21−24.
(8) Kochkar, H.; Figueras, F. *J. Catal.* **1997**, *171*, 420−430.
(9) Müller, C. A.; Deck, R.; Mallat, T.; Baiker, A. *Top. Catal.* **2000**, *11/12*, 369−378.
(10) Sever, R. R.; Root, T. W. *J. Phys. Chem. B* **2003**, *107*, 4080−4089.
(11) Bellussi, G.; Carati, A.; Clerici, M. G.; Maddinelli, G.; Millini, R. *J. Catal.* **1992**, *133*, 220−230.
(12) Barker, C. M.; Kaltsoyannis, N.; Catlow, C. R. A. *Stud. Surf. Sci. Catal.* **2001**, *135*, 2580−2587.
(13) Barker, C. M.; Gleeson, D.; Kaltsoyannis, N.; Catlow, C. R. A.; Sankar, G.; Thomas, J. M. *Phys. Chem. Chem. Phys.* **2002**, *4*, 1228−1240.
(14) Karlsen, E.; Schöffel, K. *Catal. Today* **1996**, *32*, 107−114.
(15) Neurock, M.; Manzer, L. E. *Chem. Commun.* **1996**, 1133−1134.
(16) Vayssilov, G. N.; van Santen, R. A. *J. Catal.* **1998**, *175*, 170−174.
(17) Tantanak, D.; Vincent, M. A.; Hillier, I. H. *Chem. Commun.* **1998**, 1031−1032.
(18) Yudanov, I. V.; Gisdakis, P.; Valentin, C. D.; Rösch, N. *Eur. J. Inorg. Chem.* **1999**, 2135−2145.
(19) Sinclair, P. E.; Catlow, C. R. A. *J. Phys. Chem. B* **1999**, *103*, 1084−1095.
(20) Munakata, H.; Oumi, Y.; Miyamoto, A. *J. Phys. Chem. B* **2001**, *105*, 3493−3501.
(21) Frisch, M. J.; Trucks, G. W.; Schlegel, H. B.; Scuseria, G. E.; Robb, M. A.; Cheeseman, J. R.; Zakrzewski, V. G.; Montgomery, J. A., Jr.; Stratmann, R. E.; Burant, J. C.; Dapprich, S.; Millam, J. M.; Daniels, A. D.; Kudin, K. N.; Strain, M. C.; Farkas, O.; Tomasi, J.; Barone, V.; Cossi, M.; Cammi, R.; Mennucci, B.; Pomelli, C.; Adamo, C.; Clifford, S.; Ochterski, J.; Petersson, G. A.; Ayala, P. Y.; Cui, Q.; Morokuma, K.; Malick, D. K.; Rabuck, A. D.; Raghavachari, K.; Foresman, J. B.; Cioslowski, J.; Ortiz, J. V.; Stefanov, B. B.; Liu, G.; Liashenko, A.; Piskorz, P.; Komaromi, I.; Gomperts, R.; Martin, R. L.; Fox, D. J.; Keith, T.; Al-Laham, M. A.; Peng, C. Y.; Nanayakkara, A.; Gonzalez, C.; Challacombe, M.; Gill, P. M. W.; Johnson, B. G.; Chen, W.; Wong, M. W.; Andres, J. L.; Head-Gordon, M.; Replogle, E. S.; Pople, J. A. *Gaussian 98*, revision A.9; Gaussian, Inc.: Pittsburgh, PA, 1998.
(22) NBO 5.0. Glendening, E. D.; Badenhoop, J. K.; Reed, A. E.; Carpenter, J. E.; Bohmann, J. A.; Morales, C. M.; Weinhold, F.; Theoretical Chemistry Institute, University of Wisconsin: Madison, WI, 2001.
(23) Cancès, E.; Mennucci, B.; Tomasi, J. *J. Chem. Phys.* **1997**, *107*, 3032−3041.
(24) Sastre, G.; Corma, A. *Chem. Phys. Lett.* **1999**, *302*, 447−453.
(25) Weinhold, F. A. *Encyclopedia of Computational Chemistry*; John Wiley & Sons: New York, 1998.
(26) Gonzalez, C.; Schlegel, H. B. *J. Chem. Phys.* **1989**, *90*, 2154−2161.
(27) Limtrakul, J.; Intaem, C.; Truong, T. Abstracts of Papers, 223rd ACS National Meeting, Orlando, FL, US, April 7−11, 2002; American Chemical Society: Washington, DC, 2002.
(28) Deubel, D. V. *J. Phys. Chem. A* **2001**, *105*, 4765−4772.
(29) Durant, J. L. *Computational Thermochemistry: Prediction and Estimation of Molecular Thermodynamics*; American Chemical Society: Washington, DC, 1998.